Journal of Techniques, ISSN: 2708-8383, Vol. 7, No. 3, 2025, Pages 16-25
DOI: https://doi.org/10.51173/jt.v7i3.2621

JOURNAL OF TECHNIQUES

Journal homepage: http://journal.mtu.edu.iq

RESEARCH ARTICLE - ENGINEERING (MISCELLANEOUS)

Reduce-Complexity of Predictive Current Control for a 3-Phase Voltage Source Inverter

Saif Talal Bahar[1*], Raed A. Abd-Alhmeed[2]

[1]Technical Institute / Baquba, Middle Technical University, Baghdad, Iraq

[2]School of Engineering and Informatics, University of Bradford, Bradford, U.K

[*] Corresponding author E-mail: saif.talal@mtu.edu.iq

Article Info.

Article history:

Received
07 September 2024

Accepted
21 December 2024

Publishing
30 September 2025

Abstract

This article suggests an improved simulation method for three-phase converters utilizing predictive current control. Predictive current control is a model-based on closed-loop optimization control approach. Predictive control points out without exception that the highest attractiveness of predictive control lies in its ability to handle limitations. This ability comes from its prediction of the recipient's dynamic demeanor in the system constructed on the typical by adding constraints to recipient inputs and outputs. The simulation results reveal that the suggested technique's tracking error and total harmonic distortion (THD) of the current waveform fulfill the requirements and have reasonable responsiveness. Predictive current control was employed to determine the best switching sequence for tracking errors and switching losses. The suggested approach reduces THD from (4.89%) to (1.32%). The inverter's switching states (on and off) have also been lowered using the improved method.

Publisher: Middle Technical University

Keywords: Total Harmonic Distortion; Predictive Current Control; Voltage Source Inverter; Switching Sequence.

1. Introduction

These types of current control schemes have been widely employed in power electronics and drives: hysteresis current control (HCC) [1, 2] and pulse-width modulation (PWM). Compared to HCC and PWM, the Space Vector Pulse Width Modulation (SVPWM) offers extra benefits, including greater voltage usage and reduced current ripple. However, because of its sophisticated strategy, SVPWM implementation is time-consuming [3, 4]. Model predictive current control (MPCC) has recently received much attention because of its simple idea and implementation. MPCC has demonstrated high-performance inverters [5]. Subsequently, MPCC evolved as a solid and effective technique for controlling various converters and electric motors. Predictive control refers to a broad class of controllers recently found utilization in power conversion devices.

The essential advantage of predictive control is utilizing a system model to predict the future actions of the controlled variables. The controller employs this acquaintance to limit the best actuation based on a predetermined improvement standard [6]. In hysteresis-based predictive control, the objective of the optimization is to maintain the controlled variable inside the borders of a hysteresis area, whereas, in trajectory-based control, the variables are made to comprehend a specified route [7].

The ideal actuation in deadbeat control is the person who reduces the error to zero in the following sample moments [8]. The distinction among these controller sets is that deadbeat control and MPC with a continual mechanism set require a modulation device to provide the requisite voltage, resulting in an established switching frequency [9]. The additional controls provide changeable switching frequency and the signal that switches the converter without modulation. Although MPC theory was sophisticated in the 1970s, its use in power electronics and motors is more modern because of the quick sample periods required in such structures [10]. Rapid microcontrollers made accessible in the recent decade sparked interest in innovative control techniques for power electronics and motors, such as MPC. MPC is a large relative of controllers, and various applications were suggested. An intriguing approach is the utilization of extended predictive control, which enables the improvement issue to be solved theoretically when the system is linear and there are no restrictions, resulting in an obvious surveillance rule deployed [11, 12].

This control method has been employed in several inverters [13, 14] and motor devices [15, 16]. To enable MPC implementations in an actual system, given the limited period available for computations owing to rapid sampling, it has been suggested that the majority of the improvement issues be transferred offline, utilizing an approach known as explicit MPC [17]. The MPC enhancement issue is performed offline while considering the system approach and limitations. It aims to result in a look-up table holding the best explanation as a function of the system status [18, 19]. Obvious MPC has been used to regulate power converters such as DC-to-DC inverters [20]. The resulting proximity rationalizes

Nomenclature & Symbols			
R	The load resistance	$i^{p}_{(k+2)}$	Predicts the burden of current
L	The load inductance	i^{max}	Current Limitation
$v_{\alpha\beta(k)}$	Output voltage vector	$\mathcal{g}$	Objective function
i^{*}	The orientation current	$\mathcal{g}_{\lim(k)}$	Constraint

the improvement and consents for the formulation of an explicit control rule, hence eliminating the requirement for online improvement. Nevertheless, this reduction ignores the discontinuous character of the power inverters [21].

This article aims to improve the efficiency of the 3-phase inverter under normal conditions and maintain a similar dynamic performance. The suggested method's tracking error and THD of the current waveform fulfill the requirements and have reasonable responsiveness. Predictive current control was employed to determine the best switching sequence for tracking errors and switching loss. The suggested approach reduces THD.

2. Materials and Methods

2.1. Load model

Using the variable descriptions from the circuit illustrated in Fig. 1, the formulas for burden current dynamics for each phase may be expressed as follows:

$$v_{aN} = L\frac{di_a}{dt} + Ri_a + e_a + v_{nN} \quad (1)$$

$$v_{bN} = L\frac{di_b}{dt} + Ri_b + e_b + v_{nN} \quad (2)$$

$$v_{cN} = L\frac{di_c}{dt} + Ri_c + e_c + v_{nN} \quad (3)$$

Where R is the load resistance and L is the load inductance. (e_a, e_b, e_c) Back-emf space vector, the output voltage vector can be defined as:

$$v = \frac{2}{3}(v_{aN} + av_{bN} + a^2 v_{cN}) \quad (4)$$

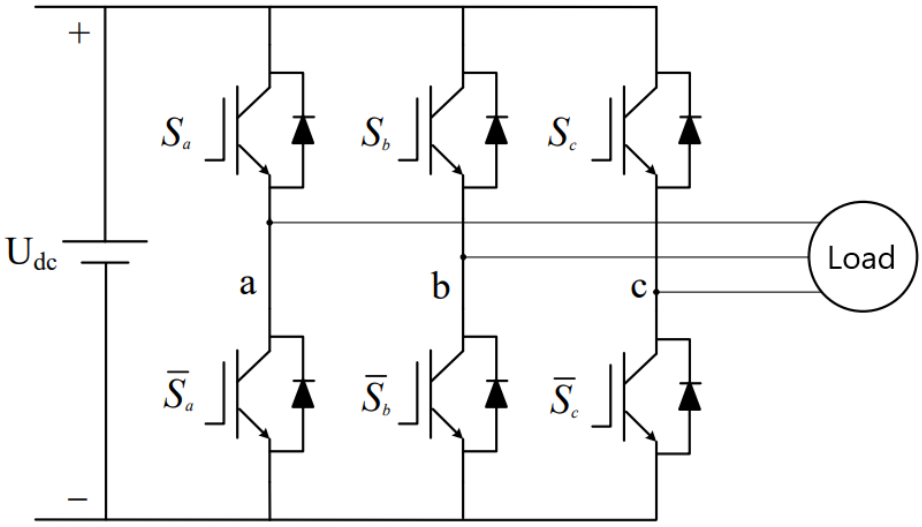

Fig. 1. Three-phase-voltage-source-inverter

These back-emf space vector definitions and load current definitions are also included.

$$i = \frac{2}{3}(i_a + ai_b + a^2 i_c) \quad (5)$$

$$e = \frac{2}{3}(e_a + ae_b + a^2 e_c) \quad (6)$$

A vector formula for the burden current dynamics canister can be acquired by substituting Eq. (1) and (2) into Eq. (4).

$$v = L\frac{d}{dt}\left(\frac{2}{3}(i_a + ai_b + a^2 i_c)\right) + R\left(\frac{2}{3}(i_a + ai_b + a^2 i_c)\right) + \frac{2}{3}(e_a + ae_b + a^2 e_c) + \frac{2}{3}(v_{nN} + av_{nN} + a^2 v_{nN}) \quad (7)$$

Subsequently, a vector differential equation can be used to describe the dynamics of the load current [22].

$$v = Ri + L\frac{di}{dt} + e \quad (8)$$

A forward Euler approximation is used in place of the burden current derivative. $\frac{di}{dt}$ In the discrete-time model for prediction [23]. Thus, the derivative is approximately represented as:

$$\frac{di}{dt} \approx \frac{i_{(k+1)}-i(k)}{T_s} \tag{9}$$

For each of the 7 voltage vector values $v_{\alpha\beta(k)}$ That the converter produces, an articulation that enables the prediction of the recipient burden current at the period $(k+1)$ must be obtained [24].(k) , $(k+1)$ present, and next values.$\alpha\beta$ coordinate this articulation is

$$i^{p}_{\alpha\beta(k+1)} = \left(1-\frac{RT_s}{L}\right) i_{\alpha\beta(k)} + \frac{T_s}{L}\left(v_{\alpha\beta(k)} - e(k)\right) \tag{10}$$

The back-emf can be projected from the equation

$$e_{(k-1)} = v_{(k-1)} - \left(\frac{L}{T_s}\right) i_{\alpha\beta(k)} - \left(R-\frac{L}{T_s}\right) i_{\alpha\beta(k-1)} \tag{11}$$

In Fig. 2, IGBT is used as a switching device, and the two switches on the same bridge arm are turned on alternately to realize the corresponding function. When the greater bridge arm switch is turned on, the corresponding smaller bridge arm switch is turned off, marked as "1"; when the greater bridge arm switch is turned off, the corresponding smaller bridge arm switch is turned on, marked as "0". Therefore, there are 8 arrangements of voltage space vectors: $U_0(000), U_1(001), U_2\ (010), U_3(011), U_4(100), U_5(101), U_6(110)\ and\ U_7(111)$, among which, except for the two vectors $U_0(000)$ and $U_7(111)$, the rest are non-zero vectors. The compound level is divided into six sectors and any vector Uref on this plane can be formed by superimposing the 8 space vectors in Fig. 2.

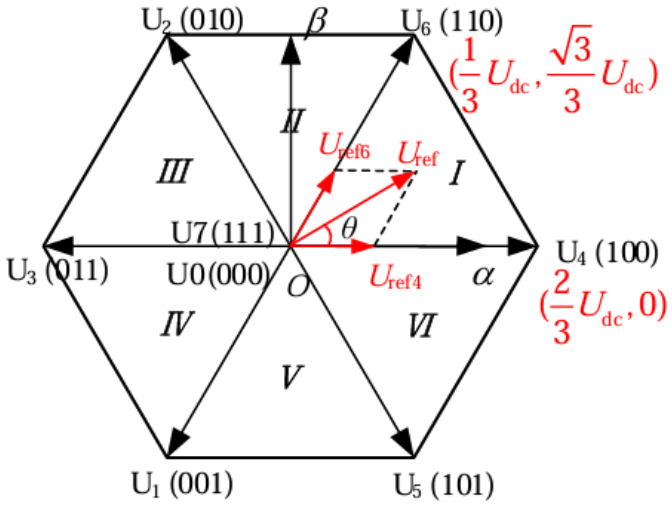

Fig. 2. Diagram of the vector selection range

2.2. Classical Predictive Current Control (PCC)

The predictive mechanism is structured on the idea that a still-inverter only produces a finite number of switching statuses and that each switching state's attitude toward the variables can be predicted utilizing models of the system [24]. It is necessary to define a selection criterion before choosing the best switching state. An objective function, which remains assessed for the anticipated values of the variables to be controlled, makes up this criterion. Fig. 3 depicts the conventional method of inverter predictive control. For each potential switching status, the predicted value of those variables is computed, and the status that reduces the objective function is then preferred.

$$g = \left|i^{*}{}_{\alpha} - i^{p}{}_{\alpha(k+1)}\right| + \left|i^{*}{}_{\beta} - i^{p}{}_{\beta(k+1)}\right| \tag{12}$$

Where i^{*} represents the orientation value and i^{p} Represents the predictive value.

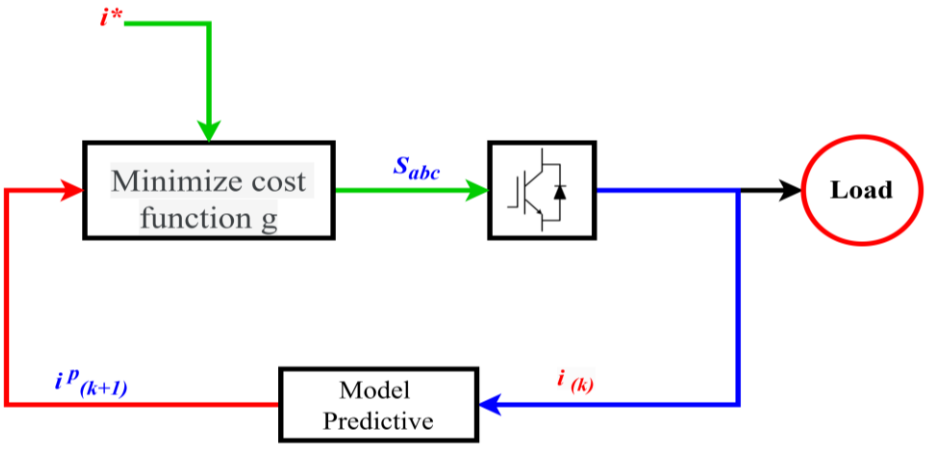

Fig. 3. Classical Predictive Current Control

2.3. Enhanced predictive current control

Voltage vectors are examined in two circumstances where two steps are evaluated for prediction. In the first scenario, one voltage vector is utilized throughout the first sample time and another during the second sampling period. This necessitates many computations, which might make the experimental implementation of the method challenging. In the second instance, the same voltage vector is utilized throughout two sample times to decrease the number of computations. The algorithm is simplified because of this technique. Fig. 4 shows the suggested scheme.

2.3.1 Enhanced PCC procedure

- Determine the value of the orientation current $i^*_{(k)}$.
- The system theory predicts the burden current for any voltage vector in the sample period $i^p_{(k+2)}$.
- For each voltage vector, the cost function g computes the difference amid the reference and anticipated currents in the following sample period.
- The voltage-reducing current error is chosen and switching status indications remain.

Fig. 5 shows the flowchart for Enhanced Predictive Current Control. To enhance the approach, current limits were implemented. Peak Current Limitation: The feedback current dynamics are neglected based on the cost functions established for the PCC schemes. The feedback current might reach the greatest threshold limit (i^{max}) During transient situations. A saturation impact in PCC is produced by establishing a nonlinear sub-cost function, as shown below.

$$g_{\lim(k)} = \begin{cases} \infty, & if \ \ |{i_{\alpha\beta}}^p| > i^{max} \\ 0, & if \ \ |{i_{\alpha\beta}}^p| \le i^{max} \end{cases} \tag{13}$$

$$i^p_{\alpha\beta(k+2)} = \left(1 - \frac{RT_s}{L}\right) i_{\alpha\beta(k+1)} + \frac{T_s}{L}\left(v_{\alpha\beta(k)} - e(k)\right) \tag{14}$$

Variations from the orientation value, as indicated in the objective function:

$$g = \left|{i^*}_\alpha - {i^p}_{\alpha(k+2)}\right| + \left|{i^*}_\beta - {i^p}_{\beta(k+2)}\right| + g_{\lim(k)} \tag{15}$$

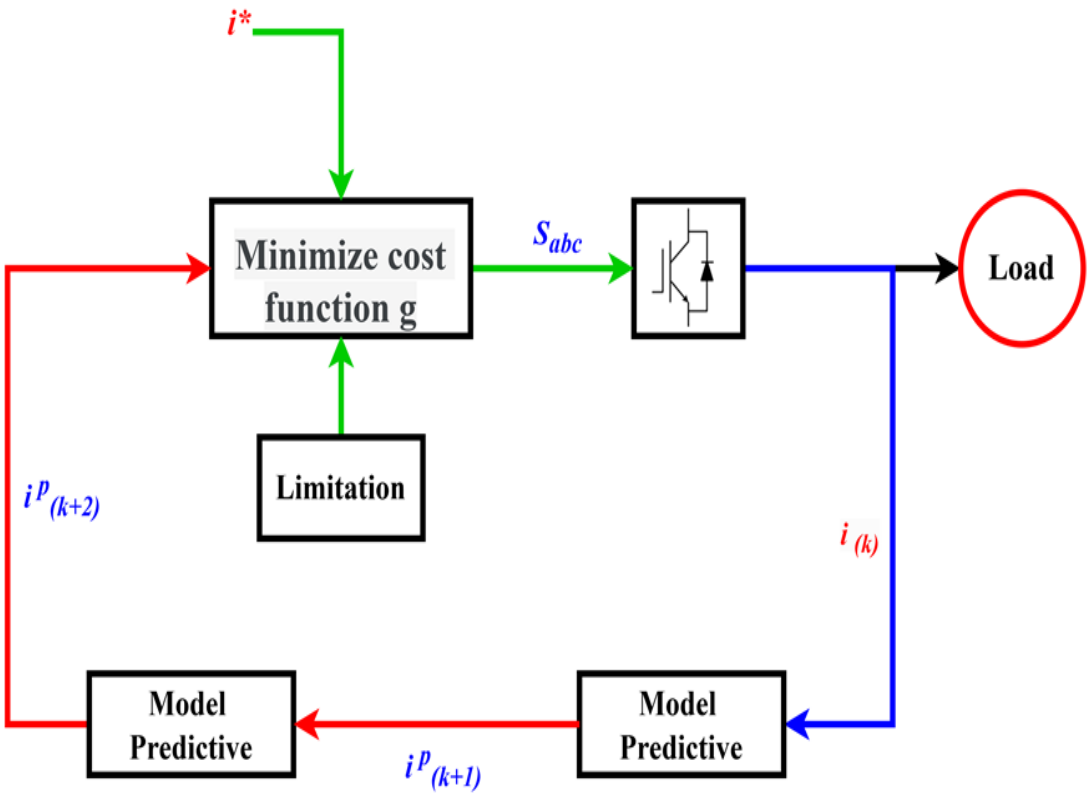

Fig. 4. Enhanced Predictive Current Control

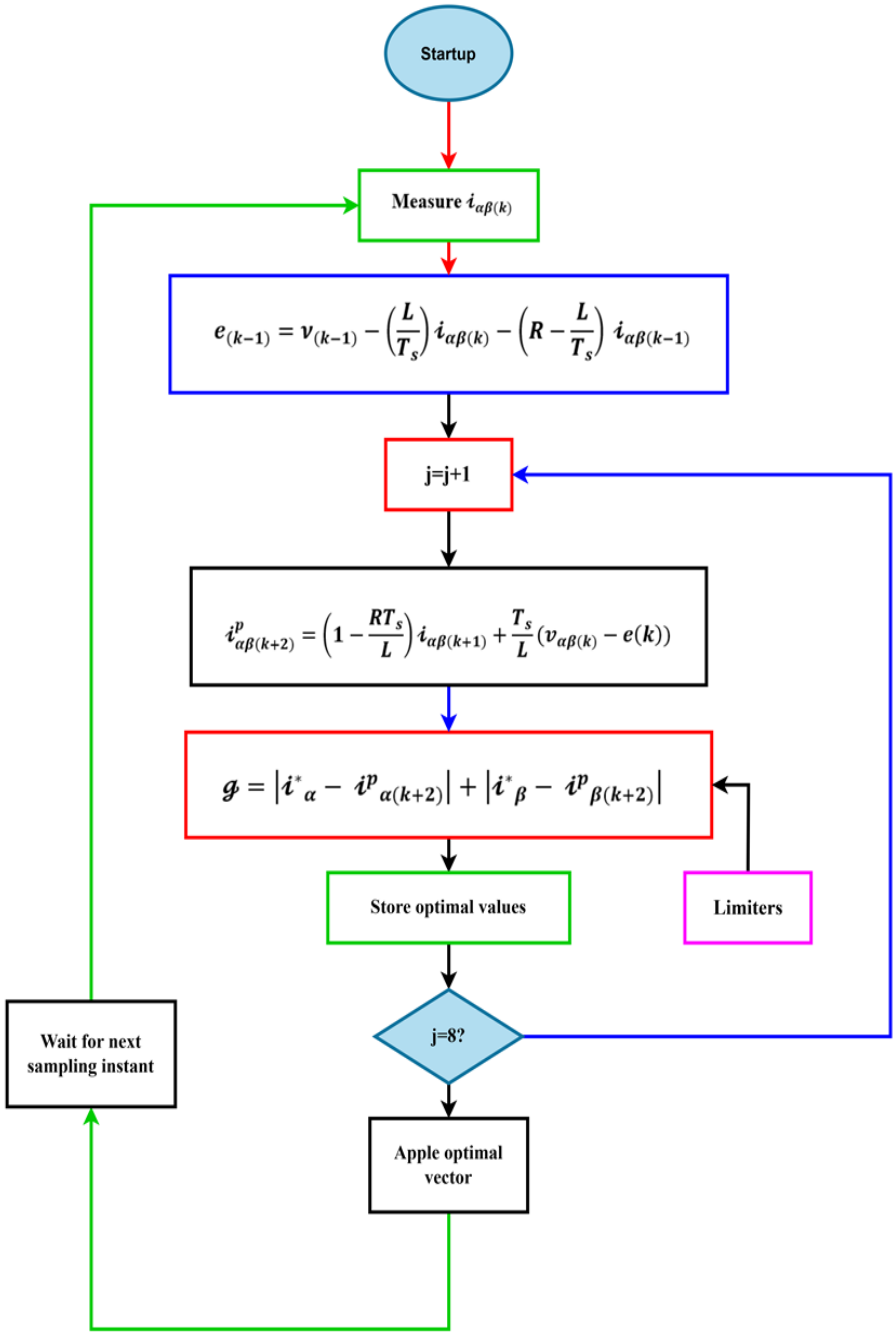

Fig. 5. Show flowchart to Enhanced PCC

3. Results and Discussion

Table 1 displays the system's parameters. To validate the suggested control approach, resistive and inductive simulations of the model presented in Fig. 6 were performed using Matlab / Simulink. This system consists of (4) subsystems and (1) MATLAB Function as follows: Orientation Current, Current Design, Inverter, switching state.

Table 1. Displays the system parameters

Parameter	Value
DC link voltage	520V
R_{Load}	10 Ω
back-EMF	100V
Sampling time	1 µsec
L_{Load}	10 mH
Frequency	50Hz

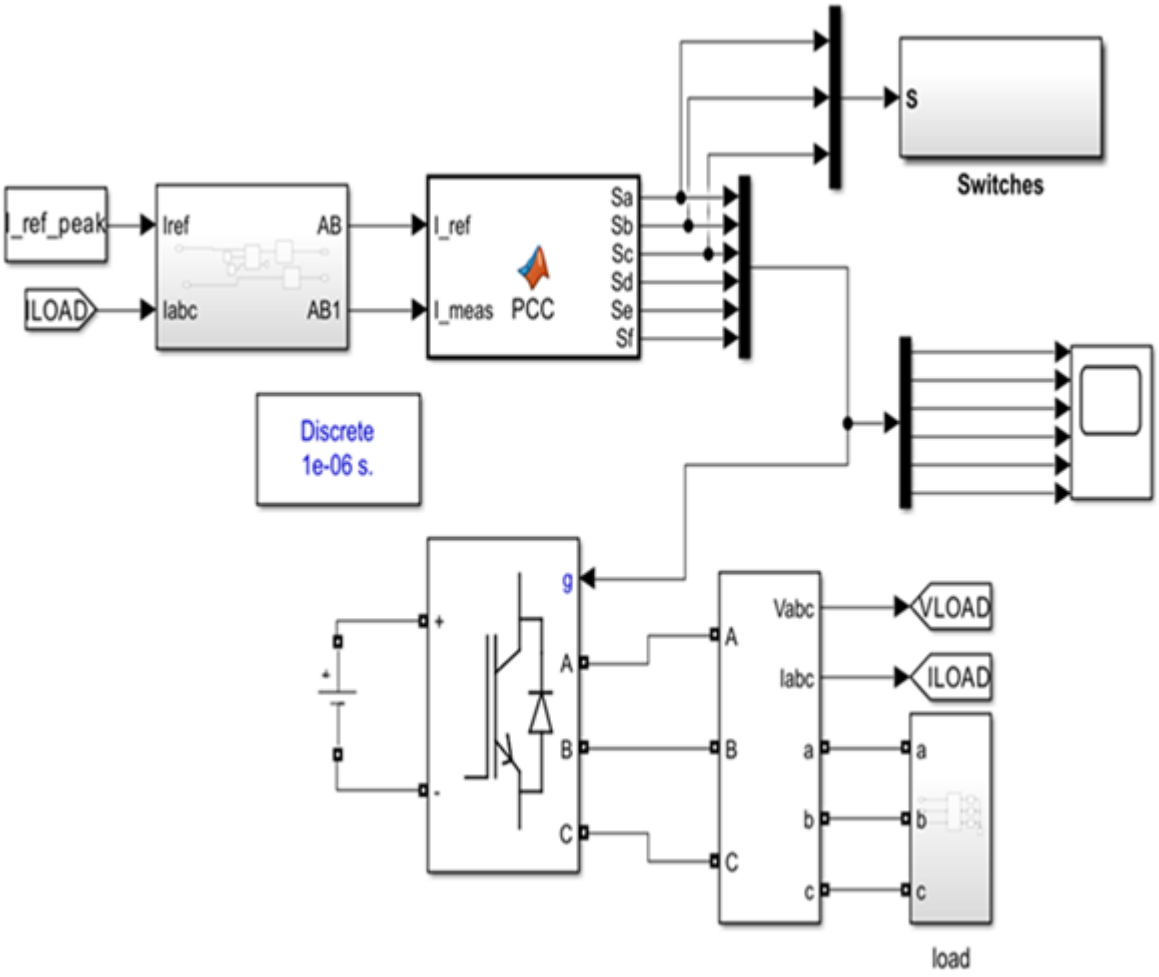

Fig. 6. Enhanced PCC

Fig. 7 depicts the steady-state 3-phase output currents of classical predictive current control (PCC). The current distortion in classical predictive current control (PCC) is high. THD for three-phase output currents is shown in Fig. 8. Under load conditions, we can see from Fig. 7 that the output current of the conventional solution has large harmonics and that the current harmonic distortion rate is 4.89%.

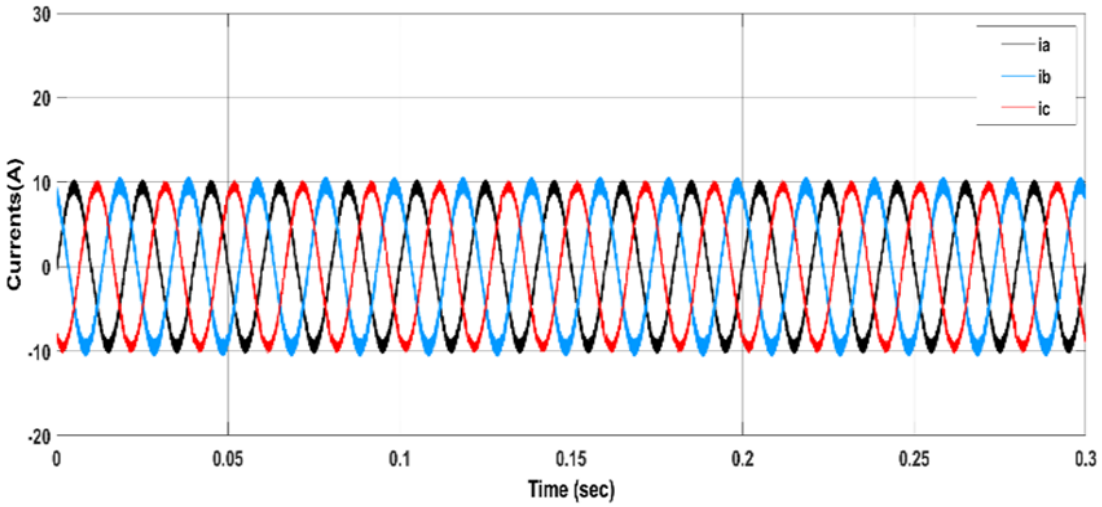

Fig. 7. Depicts 3-phase output currents in classical (PCC)

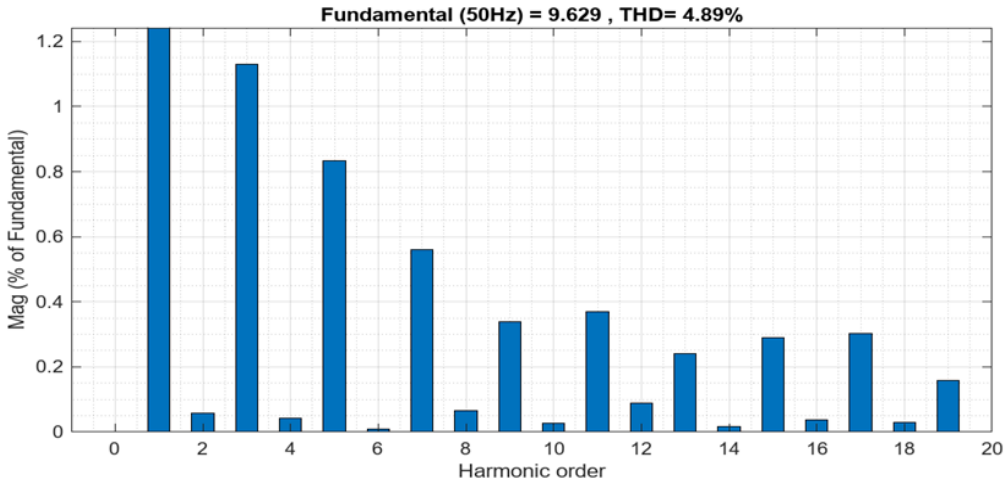

Fig. 8. Depicts THD in Classical (PCC)

Fig. 9 depicts the steady state, three-phase output currents of enhanced PCC. Consequently, the 3-phase output currents have an excellent sine wave, and the distortion has been virtually totally removed, resulting in generally smooth waveforms. THD for three-phase output currents is shown in Fig. 10. Under load conditions, we can see from Fig. 3 that the output current of the enhanced solution has low harmonics and that the current harmonic distortion rate is 1.32%.

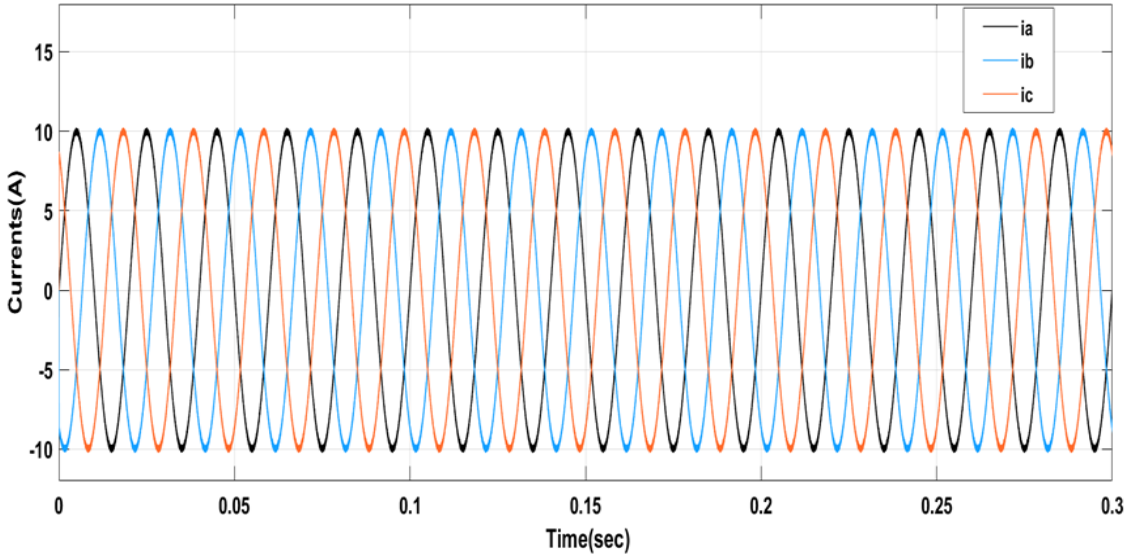

Fig. 9. Depicts 3-phase output currents in enhanced (PCC)

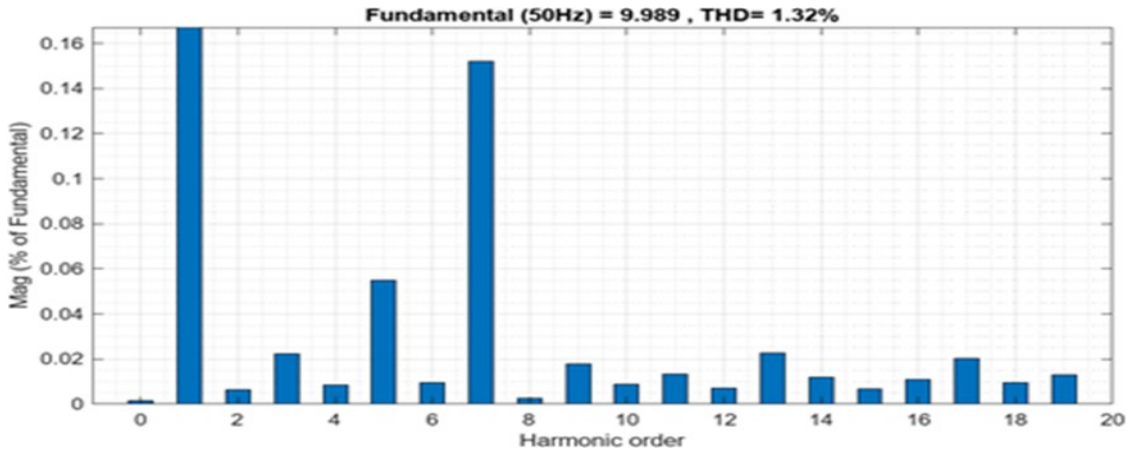

Fig. 10. Depicts THD in enhanced (PCC)

Figs. 11 and 12 depict the switches subsystem in classical and enhanced PCC, which includes the MATLAB function. This function creates all possible switching states (ON and OFF) of the PCC technique. Because of refining the suggested approach after adding limits, the number of cases (ON and OFF) in the proposed approach is smaller than the previous approach.

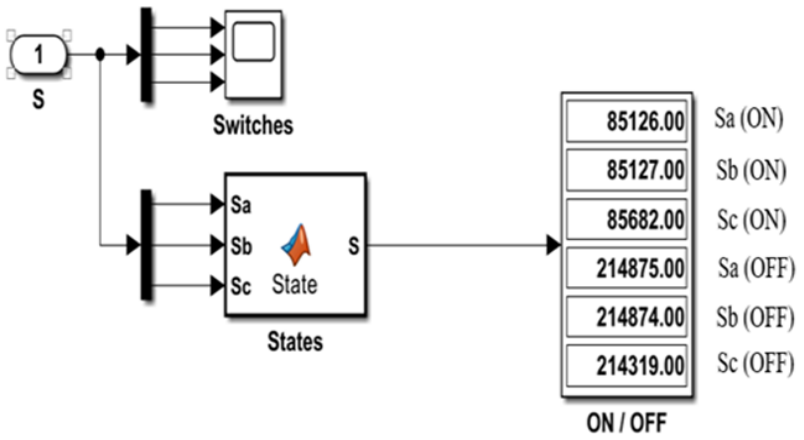

Fig. 11. Number of (ON/ OFF) changes in switching state enhanced (PCC) at (t=0.3s)

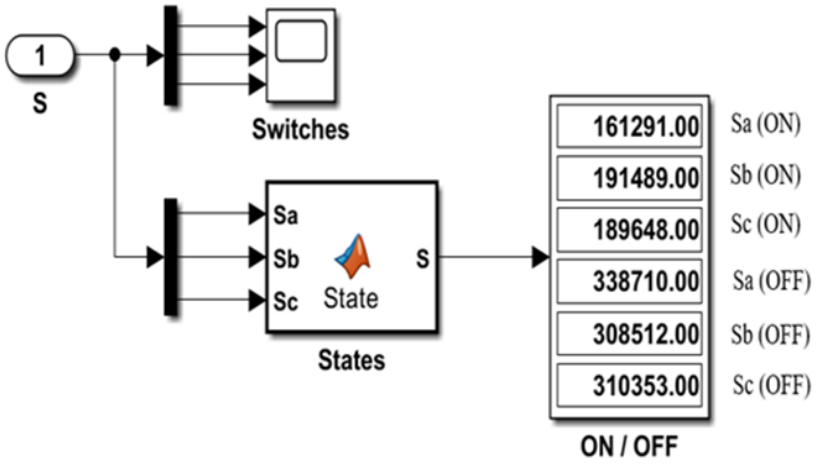

Fig. 12. Number of (ON/ OFF) changes in switching state classical (PCC) at (t=0.3s)

Figs. 13 and 14 showed the current errors between the reference's current, measured current for each phase for Classical (PCC), and enhanced (PCC). As you can observe, the error values in the previous technique vary from 1.6 to -1.6, but the error values in the modified technique range from 0.33 to -0.33, demonstrating that the enhanced approach produces good results.

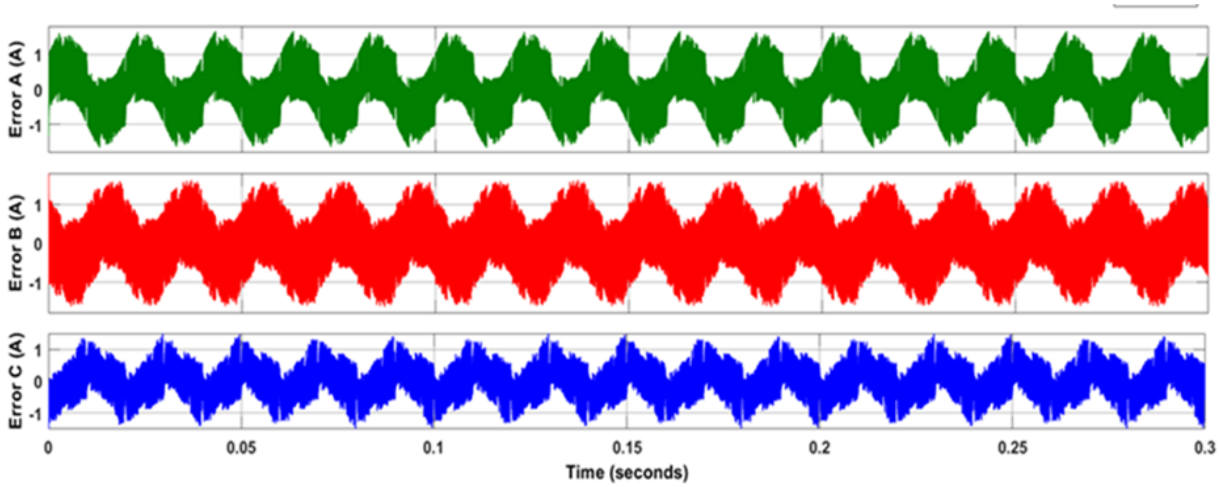

Fig. 13. Current Errors for Classical (PCC)

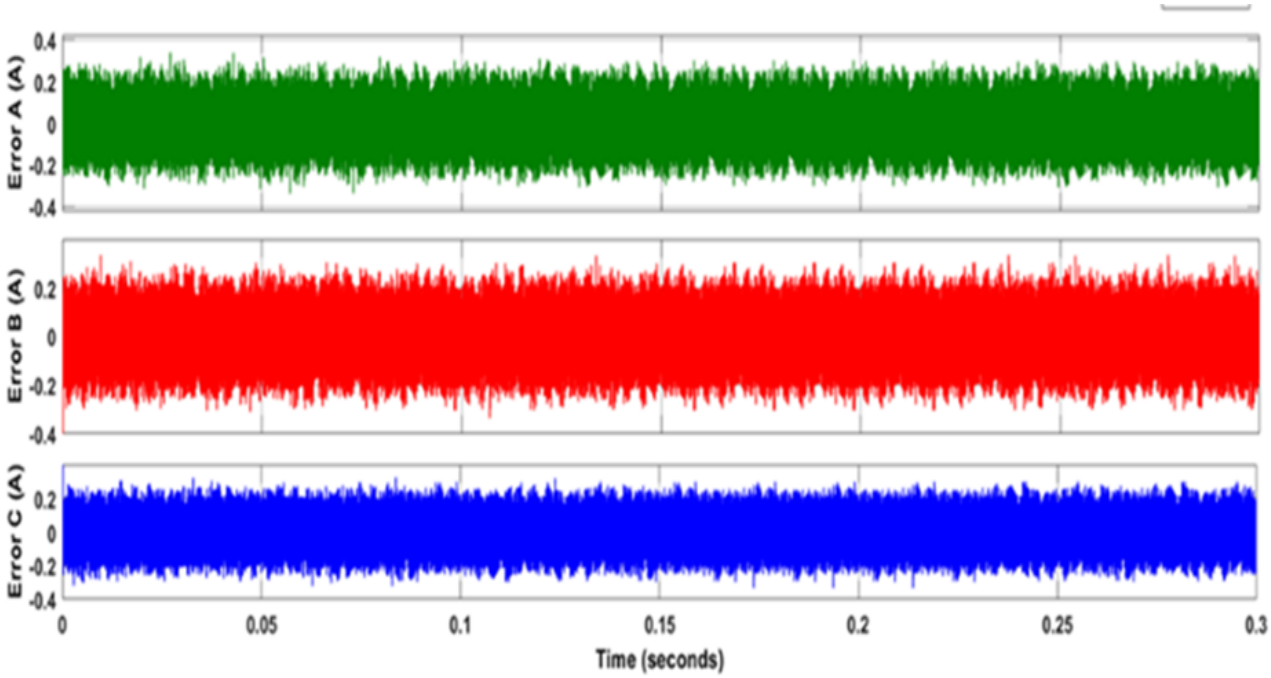

Fig. 14. Current Errors for Enhanced (PCC)

Table 2 compares classical (PCC) and enhanced (PCC).

Table 2. A compares classical (PCC) and enhanced (PCC)

Results	Classical (PCC)		Enhanced (PCC)	
THD %	4.89%		1.32%	
Current Error Value (A)	Max	1.666	Max	0.3386
	Min	-1.666	Min	-0.3386
Current Error Value (B)	Max	1.63	Max	0.3357
	Min	-1.63	Min	-0.3358
Current Error Value (C)	Max	1.495	Max	0.3241
	Min	-1.495	Min	-0.3343
Number of ON state	Sa	161291	Sa	85126
	Sb	191489	Sb	85127
	Sc	189648	Sc	85682
Number of off-state	Sa	338710	Sa	214875
	Sb	308512	Sb	214874
	Sc	310353	Sc	214319
Current error	Good		Better	

4. Conclusion

This article proposes enhancing the efficiency of the 3-phase inverter while maintaining dynamic performance. PCC features excellent control and strong robustness. It can overcome the procedure's unpredictability, nonlinearity, and analogy and handle different limitations in its controllable and manipulated variables. The simulation results reveal that the suggested technique's tracking error and harmonic distortion of the current waveform fulfills the requirements and has reasonable responsiveness. Predictive current control was employed to determine the best switching sequence for tracking errors and switching loss. The number of cases (ON and OFF) in the suggested approach is smaller than the classical approach. The proposed approach reduces THD from (4.89%) to (1.32%).

Acknowledgment

We are grateful to the lecturers at the Technical Institute / Baquba, Middle Technical University, Baghdad, Iraq, for their support in completing this academic study.

References

[1] S. Zhou, M. Zhu, J. Lin, P. G. Ipoum-Ngome, D. L. Mon-Nzongo and T. Jin, "Discrete space vector modulation and optimized switching sequence model predictive control for three-level voltage source inverters," in Protection and Control of Modern Power Systems, vol. 8, no. 4, pp. 1-16, October 2023, https://doi: 10.1186/s41601-023-00337-3.

[2] S. Yan, Y. Yang, S. Y. Hui, and F. Blaabjerg, "A Review on Direct Power Control of Pulsewidth Modulation Converters," in IEEE Transactions on Power Electronics, vol. 36, no. 10, pp. 11984-12007, Oct. 2021, https://doi: 10.1109/TPEL.2021.3070548.

[3] Y. Huang et al., "Analytical Characterization of CM and DM Performance of Three-Phase Voltage-Source Inverters Under Various PWM Patterns," in IEEE Transactions on Power Electronics, vol. 36, no. 4, pp. 4091-4104, April 2021, https://doi: 10.1109/TPEL.2020.3024836.
[4] A. Edpuganti, V. Khadkikar, H. Zeineldin, M. S. Elmoursi and M. Al Hosani, "New Submodule Selection Algorithm for Low Device Switching Frequency Modulation of Medium-Voltage Modular Multilevel Converter," 2020 IEEE International Conference on Industrial Technology (ICIT), Buenos Aires, Argentina, 2020, pp. 505-510, https://doi: 10.1109/ICIT45562.2020.9067187.
[5] W. Jiang, X. Ding, Y. Ni, J. Wang, L. Wang, and W. Ma, "An Improved Deadbeat Control for a Three-Phase Three-Line Active Power Filter with Current-Tracking Error Compensation," in IEEE Transactions on Power Electronics, vol. 33, no. 3, pp. 2061-2072, March 2018, https://doi: 10.1109/TPEL.2017.2693325.
[6] Ajel, Ahmed Rashid. "Modifying Hybrid Multilevel Inverter Employing By Using PWM and PI control techniques." Journal of Engineering and Sustainable Development 20.3 (2016): 121-128.
[7] Turki Khawish Hassan, Zainab Mahmood Abed, V/f Speed control of five-phase permanent magnet synchronous motor fed by indirect matrix converter with carrier-based PWM, Journal of Engineering and Sustainable Development: Vol. 23 No. 2 (2019): Journal of Engineering and Sustainable Development. https://doi.org/10.31272/jeasd.23.2.12.
[8] C. H. Van Der Broeck, S. A. Richter, J. V. Bloh and R. W. De Doncker, "Methodology for analysis and design of discrete-time current controllers for three-phase PWM converters," in CPSS Transactions on Power Electronics and Applications, vol. 3, no. 3, pp. 254-264, Sept. 2018, https://doi: 10.24295/CPSSTPEA.2018.00025.
[9] S. Talal Bahar and Y. G. Rashid, "A Study on an MPPT Control Approach Using Artificial Intelligence and the Perturb and Observe Method", DJES, vol. 17, no. 2, pp. 131–143, Jun. 2024, https://doi.org/10.24237/djes.2024.17210.
[10] S. T. Bahar and R. Ghanem Omar, "Permanent magnet synchronous motor torque ripple reduction using predictive torque control", J. eng. Sustain. Dev., vol. 27, no. 3, pp. 394–406, May 2023 https://doi: 10.31272/jeasd.27.3.9.
[11] C Alkorta, Patxi, et al. "Effective generalized predictive control of induction motor." ISA transactions 103 (2020): 295-305. https://doi.org/10.1016/j.isatra.2020.04.008.
[12] R. Manikandan and R. R. Singh, "Open Switch Fault Diagnosis of VSI-fed PMSM Drive using MPC Cost Function and Burg Algorithm," 2022 IEEE 1st Industrial Electronics Society Annual On-Line Conference (ONCON), Kharagpur, India, 2022, pp. 1-6, https://doi: 10.1109/ONCON56984.2022.10126621.
[13] W. Ke, C. Zhao and D. Sun, "Switch Duty Cycle Based Model Predictive Control for Hybrid-Inverter Driven Open-Winding PMSM System," 2022 IEEE 5th International Electrical and Energy Conference (CIEEC), Nangjing, China, 2022, pp. 804-808, https://doi: 10.1109/CIEEC54735.2022.9846710.
[14] Sayed, Mahmoud A., et al. "PWM control techniques for single-phase multilevel inverter based controlled DC cells." Journal of Power Electronics 16.2 (2016): 498-511. http://dx.doi.org/10.6113/JPE.2016.16.2.498.
[15] B. Xu, Q. Jiang, W. Ji and S. Ding, "An Improved Three-Vector-Based Model Predictive Current Control Method for Surface-Mounted PMSM Drives," in IEEE Transactions on Transportation Electrification, vol. 8, no. 4, pp. 4418-4430, Dec. 2022, https://doi: 10.1109/TTE.2022.3169515.
[16] C. A. Agustin, J. -T. Yu, C. -K. Lin, J. Jai and Y. -S. Lai, "Triple-Voltage-Vector Model-Free Predictive Current Control for Four-Switch Three-Phase Inverter-Fed SPMSM Based on Discrete-Space-Vector Modulation," in IEEE Access, vol. 9, pp. 60352-60363, 2021, https://doi: 10.1109/ACCESS.2021.3074067.
[17] Bahar, S. T., & Omar, R. G. Torque ripple alleviation of a five-phase permanent magnet synchronous motor using predictive torque control method. International Journal of Power Electronics and Drive Systems, 13(4), 2207, (2022). https://doi:10.11591/ijpeds.v13.i4.pp22 07-2215.
[18] A. Beccuti, S. Mariethoz, S. Cliquennois, S. Wang, and M. Morari, "Explicit model predictive control of dc-dc switched-mode power supplies with extended Kalman filtering," IEEE Transactions on Industrial Electronics, vol. 56, no. 6, pp. 1864–1874, June 2009, https://doi: 10.1109/TIE.2009.2015748.
[19] X. Zhang and C. Zhang, "A Simple Model Predictive Control for Open Winding PMSM Based on Duty Ratio Control," 2023 IEEE 6th International Electrical and Energy Conference (CIEEC), Hefei, China, 2023, pp. 517-522, https://doi: 10.1109/CIEEC58067.2023. 10166989.
[20] P. Li, X. Huo and F. Guo, "Total Harmonic Distortion Reduction Method of Improved Finite Control Set Model Predictive Control for Single-Phase Inverter with Twisted Parameter," 2023 5th International Conference on Power and Energy Technology (ICPET), Tianjin, China, 2023, pp. 284-289, https://doi: 10.1109/ICPET59380.2023.10367520.
[21] H. Miranda, P. Co´rtes, J. Yuz, and J. Rodríguez, "Predictive torque control of induction machines based on state-space models," IEEE Transactions on Industrial Electronics, vol. 56, no. 6, pp. 1916–1924, June 2009, https://doi: 10.1109/TIE.2009.2014904.
[22] Omar, Riyadh G. "Coast function parameters optimization for DC battery source inverter feeding three-phase inductive load." International Journal of Power Electronics and Drive Systems (IJPEDS) 11, no. 4 (2020): 1799-1804, https://doi:10.11591/ijpeds.v11.i4.pp1799-1804.
[23] Abdullah, Ahmad Takiyuddin, Sevia Mahdaliza Idrus, and Shahrin Md Ayob. "Model predictive control using Euler method for switched-battery boost-multilevel inverter." International Journal of Power Electronics and Drive Systems (IJPEDS) 14.3 (2023): 1497-1508, https://doi: 10.11591/ijpeds. v14.i3.
[24] S. Talal Bahar and D. Rahman Neama, "Improved Direct Torque Control Utilizing Model Predictive Control Approach for Permanent Magnet Synchronous Motor", IJSER, vol. 3, no. 2, pp. 57–64, Jun. 2024. https://doi.org/10.58564/IJSER.3.2.2024.179.